Adverse cardiovascular effects of exposure to cadmium and mercury alone and in combination on the cardiac tissue and aorta of Sprague-Dawley rats

Sandra Arbi[1], Megan Jean Bester[1], Liselle Pretorius[1], Hester Magdalena Oberholzer[1]

[1]*Department of Anatomy, Faculty of Health Sciences, University of Pretoria, Private Bag x323, Arcadia, 0007, South Africa*

Abstract

The aim of this study was to identify cardiovascular effects of relevant concentrations of Cd and Hg alone and in combination as a mixture in water. This was achieved by administering to male Sprague-Dawley rats via gavage 0.62 mg/kg Cd or 1.23 mg/kg Hg, or a combination of 0.62 mg/kg Cd and 1.23 mg/kg Hg in the co-exposure group for 28 days. Concentrations were the rat equivalence dosages of 1000 times the World Health Organization's limits of 0.003 mg/L and 0.006 mg/L for Cd and Hg respectively, for water. With termination, blood levels of the metals were increased. For all metal exposed groups, histological evaluation and transmission electron microscopy of the myocardium revealed myofibrillar necrosis, increased fibrosis, vacuole formation and mitochondrial damage. Cd caused the most mitochondrial damage while Hg to a greater degree induced fibrosis. In the aorta, both Cd and Hg also increased collagen deposition adversely altering the morphology of the fenestrated elastic fibres in the tunica media. Co-exposure resulted in increased cardiotoxicity with increased mitochondrial damage, fibrosis and distortion of the aortic wall as a result of increased collagen deposition, as well as altered elastin deposition, fragmentation and interlink formation. These are typical features of oxidative damage that correlates with a phenotype of premature ageing of the CVS that potentially can lead to hypertension and premature cardiac failure.

*** Address correspondence to** H.M. Oberholzer, Department of Anatomy, Faculty of Health Sciences, University of Pretoria Private Bag x323, Arcadia 0007, South Africa. Phone: 0123192533, E-mail: nanette.oberholzer@up.ac.za.

Keywords: Environmental exposure, cadmium, mercury, heart, aorta, blood, collagen, elastin oxidative stress.

Introduction

Cardiovascular disease (CVD) is a group of diseases that include atherosclerosis and hypertension, that affects the heart and blood vessels, which eventually leads to cardiac failure. Oxidative stress and vascular inflammation have been implicated in CVD development. [1,2] Increased arterial stiffness associated with CVD is due to a decrease and increase in elastin and collagen content respectively where increased, irreversible, non-enzymatic cross linking of collagen, contributes to early vascular ageing (EVA). [3] Atherosclerotic plaque formation is characterised by vascular inflammation resulting from endothelial cell dysfunction or injury. [1] Mitochondrial dysfunction is an identified a source of oxidative damage in vascular smooth muscle cells (VSMC) [3] and cardiomyocytes. [4] Increased fibroblastic activity is linked to heart disease, extracellular matrix (ECM) remodelling, where increased collagen deposition in the myocardium, leads to fibrosis. [3-5]

Cd is a major constituent of tobacco smoke and has been identified as an underestimated risk factor for the development of CVD and is associated with cerebrovascular accident (CVA), heart failure, myocardial infarction, peripheral arterial disease (PAD) and hypertension. [6] Blood levels below the World Health Organisation's (WHO) safety standard of 0.003 mg/L Cd and 0.006 mg/L Hg have been associated with PAD. [7] In addition to tobacco smoke, plants such as vegetables can also be a major source of Cd depending on atmospheric, soil and water levels. With soil acidification Cd levels in crops such as rice, wheat and vegetables is increased. [6] Furthermore a consequence of

increased industrial activity such as mining, oral exposure to Cd contaminated water is increasing. [6]

In the circulation, Cd binds to metallothionein and irreversibly accumulates in the liver, kidneys and testes. Cd indirectly contributes to the generation of reactive oxygen species (ROS) and reactive nitrogen species (RNS), by decreasing the available antioxidant enzymes, catalase (CAT), superoxide dismutase (SOD), glutathione peroxidase (GPx), and metabolites such as glutathione (GSH) by chelation.[6] The consequence is enzyme inactivation, pathway inhibition leading to increased ROS levels that induces oxidative damage causing increased lipid peroxidation, protein carbonylation, and DNA damage that induces inflammation and apoptosis. [6] Cd triggers an inflammatory response through the upregulation of pro-inflammatory proteins NFκB, inducible nitric oxide synthase (iNOS), COX-2 and c-myc and downregulation of anti-inflammatory cytokine interleukin (IL)-10 and heme oxygenase (HO)-1. [6] The CVS effects of Cd is the consequence of the multiple effects on the vascular endothelium and smooth muscle, mediated by the generation of a pro-inflammatory state, [6] endothelium dysfunction and down regulation of nitric oxide (NO) production, [8] and increased oxidative stress. [6]

Increased mortality of miners from the Almadén region of Spain has been identified due to Hg exposure which has contributed to circulatory diseases specifically hypertension and CVD. [9] Identified sources includes water contamination due to gold mining, leaching due to deforestation and the consumption of fish in which Hg has bio accumulated. In artisanal gold mining, Hg is used for processing of gold alluvial deposits and subsequently Hg escapes into the atmosphere and then accumulates the surrounding soils and water. With soil contamination elemental Hg is converted to inorganic Hg or converted by sulphate reducing bacteria to MeHg which is absorbed by plants, often consumed by humans. [10] In Brazil, artisanal gold miners are exposed to Hg while local communities are exposed via atmospheric vapour inhalation and ingestion of Hg contaminated fish. [10]

In the blood Hg is widely distributed to other tissues where it binds to sulfhydryl groups such as the Cys residues of proteins and GSH. Inorganic mercury such as $HgCl_2$ has low lipophilicity, which limits its ability to penetrate through the blood brain barrier. Once absorbed, Hg undergoes metallic interconversion where organic methyl-Hg is converted to inorganic Hg in the kidneys and the liver as a result of microbial flora activity. Hg is oxidized by erythrocytes to Hg^{2+} which binds to SH-groups altering the tertiary and quaternary structure of proteins, the catalytical activity of enzymes, disrupts receptor binding and subsequent changes in K^+ or Ca^{2+} levels alters cell membrane potentials and intra- and intercellular signalling. [10, 11]

Due to its high affinity for SH-groups, ionic Hg binds to GSH, Cys, homocysteine, *N*-acetylcysteine, metallothionein, as well as albumin, inhibits SOD, CAT and GPx, adversely altering antioxidant status of cells and tissue. [10,11] In the mitochondria Hg disrupts mitochondrial enzyme systems and this leads to depolarisation, autoxidation and peroxidation of the inner mitochondrial membrane. Reduced integrity of the inner mitochondrial membrane alters calcium homeostasis, causes an increase in H_2O_2 levels, and depletes GSH, increases lipid peroxidation and oxidation of cofactors NADH and NADPH. [11] Oxidative stress and depletion of mitochondrial oxidant defence mechanisms has a detrimental effect on the functioning of mitochondrial rich tissue types such as cardiac and smooth muscle. [12]

Methylmercury levels lower than that associated with neurotoxicity has been identified to increase the progression of atherosclerosis and risk for CVD. [10] The vascular effects of Hg, include increased oxidative stress and inflammation, depletion of oxidative defence mechanisms, and also causes vascular smooth muscle, endothelial, immune and mitochondrial dysfunction. [10, 11]

Although studies have investigated the effects of heavy metals and their combinations both *in vitro* and *in vivo,* [13-15] no studies could be identified on the effects of Hg and Cd alone and in combination on the CVS. Only effects of these metals on several blood parameters [15, 16] have been investigated.

Compromised antioxidant defence systems were observed in workers exposed chronically to Cd and Hg in coal fly-ash where exposure adversely affected plasma levels of ascorbic acid SOD and GPx, increasing the risk for oxidative stress. [17] Although smoking and exposure to Cd and Hg are associated with the development of hypertension and CVD, [10, 11, 18-20] little is known whether oral exposure at concentrations that can be extrapolated to human limits for water have comparable adverse health effects on the CVS. In a Sprague-Dawley rats, the aim of this study is to firstly to evaluate the effects of oral exposure of environmentally relevant concentrations of Cd and Hg, secondly, to compare this with the effects of co-exposure to Hg and Cd as part of a mixture on the tissue and cells of the heart and aorta.

Materials and Methods

Sprague-Dawley rat model

Six-week-old, male, Sprague-Dawley rats (average weights 250 - 300 g) were maintained at the University of Pretoria Biomedical Research Centre (UPBRC). Standard irradiated Epol rat pellets and municipal water were provided *ad libitum*. The rats were housed conventionally in cages complying with the sizes laid down in the SANS 10386:2008 recommendations. A room temperature of 22ºC (± 2), relative humidity of 50% (± 20) and a 12-hour night/dark cycle was maintained throughout the study. A total of 24 rats (n=6 per group) were used in the study. The rats were housed in pairs per cage and autoclaved pinewood shavings were used as bedding material, along with white facial tissue paper as enrichment as per the standard operating procedures at the UPBCRC. All experimental protocols complied with the requirements of the University of Pretoria Animal Ethics Committee (AEC) (Animal ethics number: H007-15). The rats were divided into the experimental groups at random and allowed to acclimatise for 7 days. The rats were dosed at a 1000 times the safety limit of exposure levels established by the WHO [21] of 0.003 and 0.006 mg/L for Cd and Hg respectively. The rat equivalent dose (RED) according to Nair and Jacob (2016) was calculated. [22] Dosages was based on a human with a weight of 60 kg, consuming 2 litres of water per day were used which at 1000 times the WHO limit translates into a daily dosage of 6 and 12

mg/day (equivalent to 0.1mg/kg and 0.2 mg/kg) for Cd and Hg respectively. The RED was 0.62 and 1.23 mg/kg/day for Cd (II) and Hg (II) ions respectively. The rats were exposed via gavage daily for 28 days resulting in a control group and three experimental groups, rats exposed to Cd (Cd), Hg (Hg) and the a mixture of Hg and Cd (Cd+Hg). The rats were weighed daily prior to administration of the metals and weekly average weights of rats were used to calculate dosages. On the day of termination, the rats were terminated via isoflourane overdose according to standard methods employed by the UPBRC. Blood was collected, via cardiac puncture in citrate tubes and was sent to an external laboratory for the quantification of plasma creatinine as well as Cd and Hg, the latter determined with coupled plasma mass spectrometry. The heart and aorta were dissected from each rat. For histology the left ventricle and the upper thoracic portion of the descending aorta of all rats were collected and processed for light microscopy (LM) and transmission electron microscopy (TEM). The most representative images of each group were used to document the changes in tissue and cell structure.

Histology of cardiac tissue and the aorta

Tissue prepared for paraffin wax embedding was fixed overnight in 4% formaldehyde (FA) in 0.1M phosphate buffer saline solution (PBS) (0.2 M Na_2HPO_4, 0.2 M $NaH_2PO_4 \cdot H_2O$, 0.15 M NaCl, pH = 7.4). The samples were then washed three times for 30 minutes with PBS before being dehydrated in increasing concentrations of ethanol of 50% ethanol for 30 minutes, 70% ethanol for 1 hour, 90% ethanol for one hour, twice in 100% ethanol for one hour, and 100% ethanol overnight. The samples were then infiltrated with paraffin wax by first placing them in 50% xylene: ethanol for 30 minutes, then 100% xylene for 2 hrs, followed by 30% wax in xylene for 1 hour, 70% wax in xylene for 1 hour and finally in 100% wax for two hrs. All steps involving wax infiltration were undertaken at 60ºC. The samples were embedded in paraffin wax and cooled to 4°C

prior to sectioning. The prepared blocks were sectioned at a thickness of 3 – 5 µm using a Leica RM2255 microtome. Prior to staining, all wax sections were de-waxed in xylene and rehydrated and then dehydrated with 90% and 100% ethanol to xylene according to standard protocols after

completion of the staining. Haematoxylin and Eosin staining was undertaken as described previously. [53]

Elastic distribution: Verhoeff van Gieson stain for elastin

The distribution of elastic fibers in the aorta was evaluated with the Verhoeff van Gieson (VvG) method. Verhoeff's solution was prepared by mixing together 20 ml 5% alcoholic haematoxylin, 8 ml 10% ferric chloride, 8 ml Weigert's iodine solution, before staining for 1 hour. Differentiation was achieved by rinsing the slides in 2-3 changes of tap water and then with a 2% ferric chloride solution for 1-2 minutes. Further differentiation was achieved with several changes of tap water, after which the slides were treated with a 5% sodium thiosulfate solution for 1 minute and washed again in running tap water for 5 minutes. Counterstaining was achieved with Van Gieson's solution, consisting of 5 ml of a 1% aqueous acid fuchsin in 100 ml of a saturated aqueous picric acid solution, for 3 - 5 minutes.

Transmission electron microscopy of the heart and aorta

Transmission electron microscopy was undertaken as described previously.[23] Shortly the tissue samples were fixed in 2.5% glutaraldehyde (GA)/FA in 0.075 M phosphate buffer, pH 7.4 for 1 hour, rinsed three times in PBS for 15 minutes before being placed in a secondary fixative of 1% osmium tetroxide solution, for 1 hour. The samples were rinsed again as described above, dehydrated in 30%, 50%, 70%, 90% and three changes of 100% ethanol before being embedded in Quetol resin. Ultra-thin sections (70 - 100 nm), were cut, contrasted with uranyl acetate for 15 minutes followed by 10 minutes of contrasting with lead citrate. Finally, after drying for a few minutes the samples were examined with the JEOL JEM 2100 TEM (JEOL Ltd., Tokyo, Japan).

Statistical analysis

Statistical analysis of blood creatinine and metal levels was undertaken with One-way analysis of variance (ANOVA) and Tukey's multiple comparison test was used where a p-value of < 0.05 was considered significant.

Results and discussion

In this study the cardiovascular toxicity of Cd, Hg alone and in combination was determined 28 days after exposure. Several studies have investigated the cardiotoxicity of Cd and Hg but whether dosages used reflects human exposure is often questioned. In the present study, this was addressed by exposing rats to the RED of 1000 x the WHO limit for water for 28 days. In addition the effects of co-exposure to Hg and Cd at the same concentrations was also determined.

Creatinine levels on the day of termination were similar to the control for Cd but were significantly reduced compared to the control for Hg and co-exposed rats. For the co-exposed group, creatinine levels was significantly less that measured for Hg and Cd exposed rats. Creatinine levels serves as surrogate for muscle mass [54] which may indicate that in groups where levels are significantly lower, muscle mass may be reduced and functioning possibly compromised (Table 1).

Table 1: Creatinine and blood levels of Cd and Hg and the percentage absorption in the experimental groups after 28 days exposure.

Treatment	Creatinine	Cd (nM)	Hg (nM)	% Absorption
Control	27.17±2,22	< 4.5	< 5.0	NA
Only Cd	24.17±1.17	16.69 ± 3.69	-	19.11 ± 4.22
Only Hg	21.83±2.17*#	-	186.67 ± 22.12	43.24 ± 5.12
Cd + Hg co-exposure	12.97±12.91#	121.06 ± 140.17#	155.99 ± 41.12#	72.14 ± 83.52 and 51.75 ± 13.64 respectively

*Significant $p<0.05$, control vs Cd, Hg, Cd+Hg co-exposure, # significant Cd vs Cd+Hg and Hg vs Cd+Hg co-exposure ($p<0.05$)

Plasma levels of Cd and Hg were measured on the day of termination following 28 days exposure. The levels of Cd and Hg were 16.69 ± 3.69 nM and 186.67 ± 22.12 nM respectively and were higher than that measured in the control group. Differences between Cd and Hg and the co-exposure group was statistically significant.

Cd levels of 16.69 ± 3.69 nM, equivalent to 1.872 ± 0.37 µg/L is within ranges for several Cd exposed populations. Reported examples are 0.8 – 4.5 µg/L for an Egyptian population, [25] 0.05 – 0.258 µg/L and 0.06 – 0.39 µg/L for a female South African rural and mining community respectively, [26] and for a Swedish adult group, levels were 0.46 µg/L blood Cd [27]. The detrimental effects of Cd exposure is augmented by exposure to tobacco smoke, [28] which can increase Cd intake by an extra 1 - 3 µg Cd for individuals smoking one pack of cigarettes per day. [29] Blood levels of Cd in smokers were increased from 1.37 ± 0.45 µg/L to 2.67 ± 1.21 µg/L for an Egyptian population, [25] whereas for Canadians these levels increased from an average of 0.21 µg/L to 1.64 µg/L for smokers compared with non-smokers. [30] Although this does not represent oral exposure, it further contributes to blood levels and associated toxicity.

For Hg exposed rats, the plasma Hg levels, after oral exposure were 35.41 ± 2.60 µg/L which was higher than levels found in several populations. Plasma Hg levels were reported to be an average of 3.08 ± 1.55 µg/L for a Korean male college population (n=43) [31] and 4.6 ± 3.0 µg/L for a larger population of Korean males (n=4283). [32] In an Egyptian population, Hg levels were 4.4 – 12.1 µg/L, [28] and in a South African population 0.1 - 8.82 µg/L. [26] In the study by Röllin *et al.* (2009) levels in South African rural women were 0.18 - 8.82 µg/L while for women living in mining areas were 0.28 - 1.25 µg/L. [26] In contrast, in regions of the world where small scale gold mining occurs, serum levels of Hg were raised and increased from 16.6 ± 10.7 µg/L to 102.0 ± 55.8 µg/L for different mining areas in Ghana. An increase in cardiovascular events has been reported in populations exposed to 0.05 µM Hg, equivalent to 10.29 µg/L Hg. In the present study rat blood levels of 35.41 ± 2.60 µg/L representing the upper range of Hg exposure which is associated with

cardiovascular risk. A study in which Wistar rats treated with intramuscular $HgCl_2$ for 30 days (first dose 4.6 µg/kg, then 0.07 µg/kg/day) identified that chronic low-level Hg exposure significantly altered the autonomic modulation of heart rate through a shift towards sympathetic control and blockage of pacemaker activity of the sinoatrial node, [33] identifying cardiac tissue as a site of toxicity.

In the present study both metals were absorbed, and the percentage absorbed was 19.11 ± 4.22% and 43.24 ± 5.12% respectively for Cd and Hg. In the co-exposure group the percentage absorption for reach metal was increased to 72.14 ± 83.52 % and 51.75 ± 13.64% for Cd and Hg respectively. This is either due to an increase in total metal burden or that Cd or Hg metals alters the permeability of the intestinal mucosa, increasing absorption. Cadmium causes mild to moderate villus damage and inflammatory cell infiltration in the lamina propria [34] while a dose dependant sloughing of intestinal villi was reported with Hg exposure. [35] Either effects can increase mucosal permeability, which could account for the higher blood levels of especially Cd found in the co-exposure group.

Histology of the myocardium of the control, revealed oval centrally located nuclei. The myofibrils were striated, branched and continuous with adjacent myofibrils (Fig. 1). Small blood vessels and capillaries are often visible throughout the cardiac muscle. Distinctive and varying degrees of cardiotoxicity was observed in the experimental groups (Fig. 1) and generally the muscle tissue was irregular and loose in appearance. Deformations in size and shape of the nuclei and a disordered pattern of myofibres were common. In the Cd exposed group (Figure 1d), lipid vacuoles, flattened nuclei, destruction of myofibrils and dilatation of the cardiac tissue, often associated with tissue oedema was observed. Exposure to Hg (Fig. 1f), caused increased destruction of myofibrils, the formation of vacuoles and erythrocyte extravasation due to capillary and small blood vessel distortion or injury. In the co-exposed group (Fig.1 g and h) lipid vacuoles as well as thin filaments of connective tissue were observed (Fig.1h thin arrow).

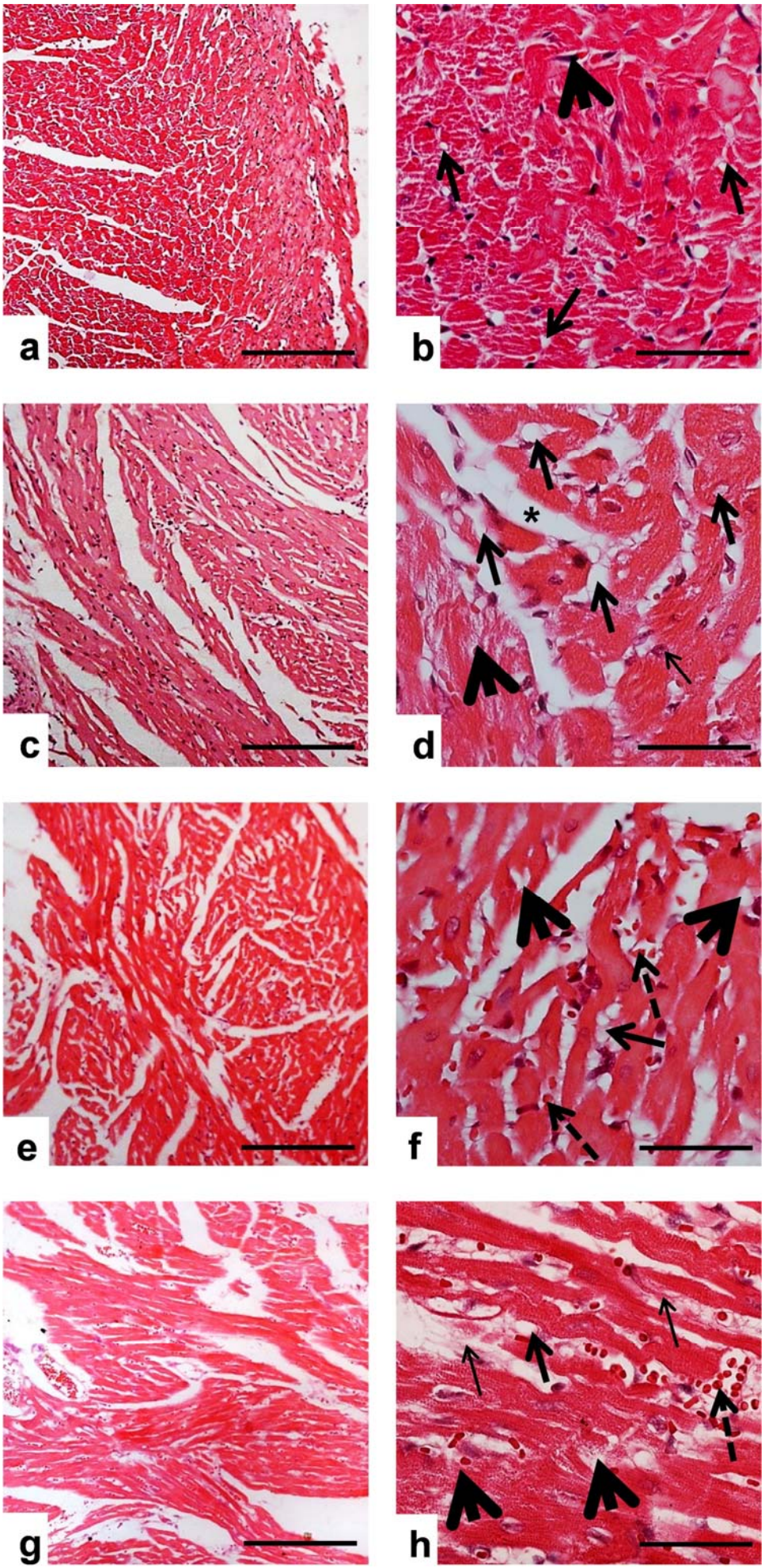
a
b
c
d
*
e
f
g
h

Figure 1: H&E stain of cardiac tissue in control sample (a) with neatly arranged myofibrils. In all heavy metal groups; Cd (c), Hg (e) and Cd+Hg (g), irregular and loose appearance of muscle tissue is visible at low magnification. At high magnification in control (b), single oval and centrally located nuclei (arrowhead) and small blood vessels and capillaries (arrows) are visible. Cd (d) shows presence of lipid vacuoles (arrow), irregular and flattened nuclei (thin arrow), destruction of myofibrils (arrowhead) and tissue dilatation (*). Further destruction of myofibrils is evident in the Hg exposed group (f) (arrowhead) with presence of lipid vacuoles (arrow), and extravasation of erythrocytes (dashed arrow). In the Cd+Hg group (h), destruction of myofibrils (arrowhead) and erythrocytes extravasation (dashed arrow) are apparent and lipid deposition (arrow) as well as fine connective tissue fibrils are also present (thin arrow). Scale bars = 5 µm.

Cd has been shown to accumulate in heart muscle [36] and is cardiotoxic at concentrations as low as 0.1 µM (equivalent to 11,24 ug/L). [37] Chronic exposure of Wistar rats to 15 mg/kg/day for 60 days resulted increased Cd accumulation in cardiac tissue resulting in altered mitochondria structure, the presence of thin and disintegrated muscle fibres, with disruption of normal myofibrillar organisation while the structure of the endothelium and SMC was normal. Ghosh and Indra [38] evaluated the effects of 5mg/kg/day for 30 days and found myofibrillar arrangement, vacuolization of the tissue and erythrocyte congestion in the cardiac tissue. Inflammation and oxidative damage to DNA, lipid and proteins as well as inhibition of the antioxidant defence mechanisms was also observed. [39] Likewise Ferramola et al. [40] describe the cardiotoxic and antioxidant pathway inhibitory effects of 15 mg/kg/day and 100 mg/kg/day administration of Cd in Wistar rats for 60 days.

Although Hg has been identified as a cardiotoxin that mediates its effect via oxidative mechanisms, few studies investigate the morphological effects on tissue and cellular structure. Baiying et al. [40] reported that blood levels of 500 µg/L after oral intake of Hg for 56 days by Wistar rats resulted in increased levels of creatine kinase (CK) and CK myocardial band isoenzyme as well as oxidative related increase in malondialdehyde (MDA) levels, reduced GSH levels and the ratio of GSH/GSSG. Morphological features of damage was haemorrhage and infiltration of inflammatory cells. The administration of 1mg/kg per day, for 28 days to Wistar rats also resulted in an increase

in MDA levels and a decrease in the levels of antioxidant enzymes in cardiac tissue. [41] These levels resulted in inflammatory cell infiltration, myocardial fibres disorganisation, myocyte degeneration, edema and necrosis. In the present study, lower blood levels of 35.41±2.60 µg/L and relevant dosages of 0.2 mg/kg resulted in milder morphological effects with the absence of inflammation and necrosis although changes to the fibre arrangement and the myocytes were observed.

In the present study, the cardiotoxicity of Cd and Hg was confirmed, however no previous reports being found on the cardiotoxic effects of co-exposure to Cd and Hg.

Following metal exposure with TEM (Fig. 2), parallel bands of mitochondria and cardiac muscle fibrils, characteristic of normal cardiac muscle (Fig. 2a, arrow), were distorted. Interruptions of Z lines were evident in the Cd exposed group together with a clear destruction of the myofibrils (Fig. 2 c and d, arrowhead), resulting in fewer myofibrils associated with swollen mitochondria (Fig. 2c and d, thin arrows). Similar myofibrillar damage was observed in the Hg group (Fig. 2f, arrowhead) and in the combination group (Fig. 2g, arrowhead). In the Hg group, damage and destruction of the mitochondria were visible as spaces and dilatations of the mitochondrial body (Fig. 2e and f, thin arrows). In the co-exposure group there were small, damaged mitochondria (Fig. 2g, dashed arrow). Interstitial collagen deposition was also present.

Exposure to low doses of Cd increases levels in cardiac tissue and dilated cardiac myopathy develops due to the effects of Cd on the cardiac endothelium, [42] via the disruption of endothelial cadherin. [43] Erythrocyte extravasation is associated with vascular leakage because of endothelial damage. Hg promotes vascular damage and leakage into tissues and consequently interstitial edema. [75] In the present study this effect was observed especially for cardiac tissue of rats exposed to Hg and with co-exposure to Cd and Hg, identifying the contribution of Hg to endothelial damage.

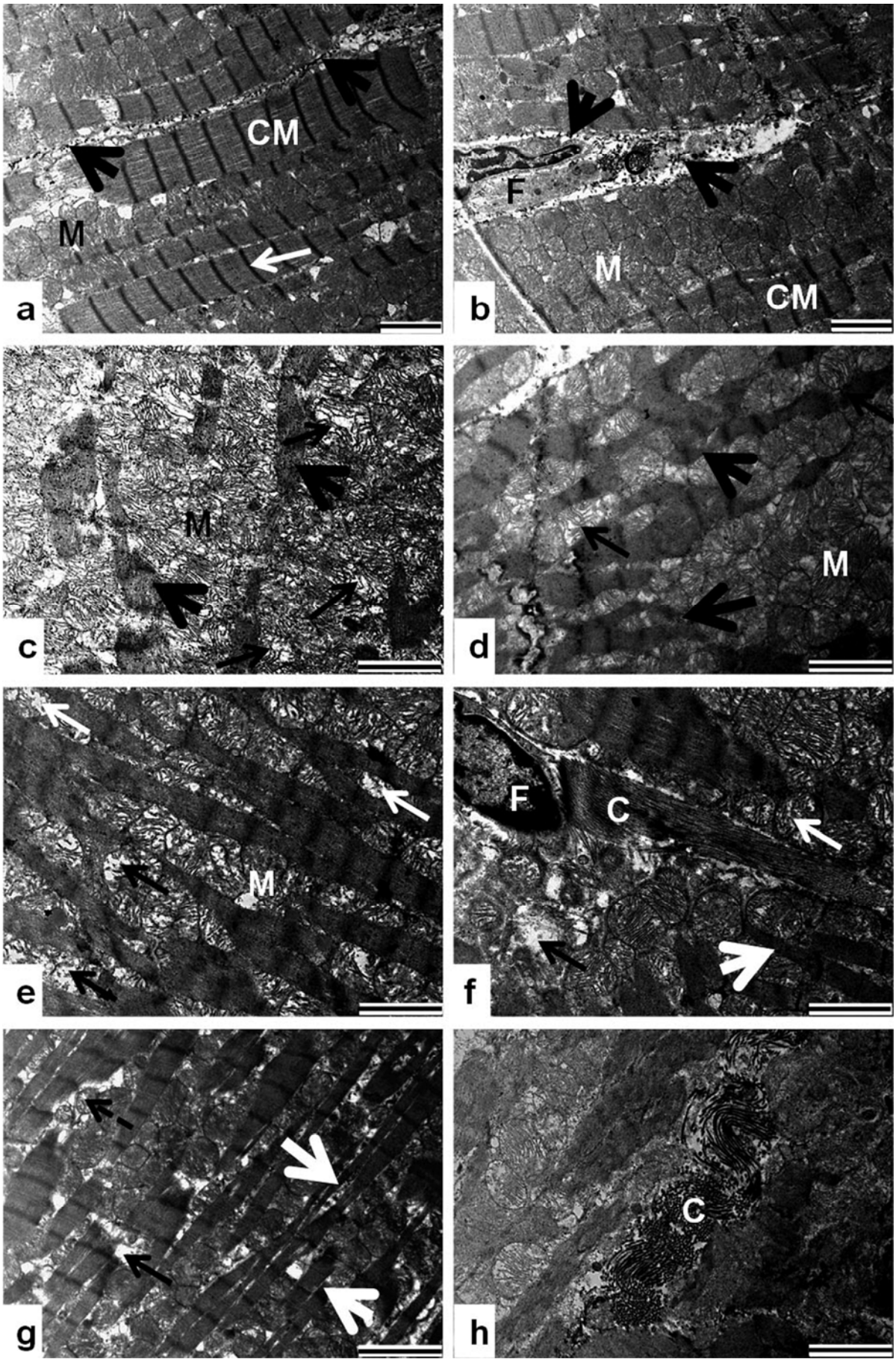
CM
M
a
F
M
CM
b
M
c
M
d
M
e
F
C
f
g
C
h

Figure 2: General ultrastructural features of cardiac muscle in control (a and b), Cd (c and d), Hg (e and f) and Cd+Hg group (g and h). Control (a) show normal ultrastructure with well organised parallel bands of mitochondria and cardiac muscle fibrils, with clear Z lines (arrow). Collagen fibrils forming part of the endomysium (arrowheads). In (b) a myofibroblast (F) is shown, with collagen fibrils surrounding it (arrowheads). Cd (c and d) shows a destruction of myofibrils (arrowheads) and areas of myofibre loss being replaced by mitochondria, which appear swollen (thin arrows). In (e and f), mitochondria appear enlarged with slight vacuolisation (arrows). In (f) thin, broken myofibrils are present (arrowheads) and very dense collagen accumulation (C) around a myofibroblast (F). Cd+Hg (g and h) group shows extensive thinning and destruction of myofibrils (arrowheads) as well as loss of myocardial tissue (arrow) and small, damaged mitochondria (dashed arrow) in (g). Interstitial collagen (C) deposition is shown in the combination group (h). Mitochondria (M), Cardiac myofibrils (CM), myofibroblast (F), Collagen (C). Scale bars = 2 μm.

In the present study changes to the mitochondrial size and the cristae of the compared with control group was also observed (Fig. 3). In the control group the mitochondrial cristae are neatly and closely packed (Fig. 3a) and the empty spaces visible in the tissue (indicated by the arrow), are axial tubules. Infrequent alterations to the structure of the mitochondrial cristae was observed in the controls. In the exposed groups, mitochondrial damage occurred. In the Cd exposed group swelling and slight damage to the mitochondrial cristae (Fig. 3b, arrows) was observed. The destruction of cristae was observed in the mitochondria of the Hg group (Fig. 3c, arrow) although the frequency of damaged mitochondria was less than that observed in the Cd group. Following co-exposure to Cd and Hg (Fig. 3d), increased mitochondrial toxicity was observed, with either extensive swelling of the mitochondrial matrix, or complete loss of cristae (Fig. 3d, arrows).

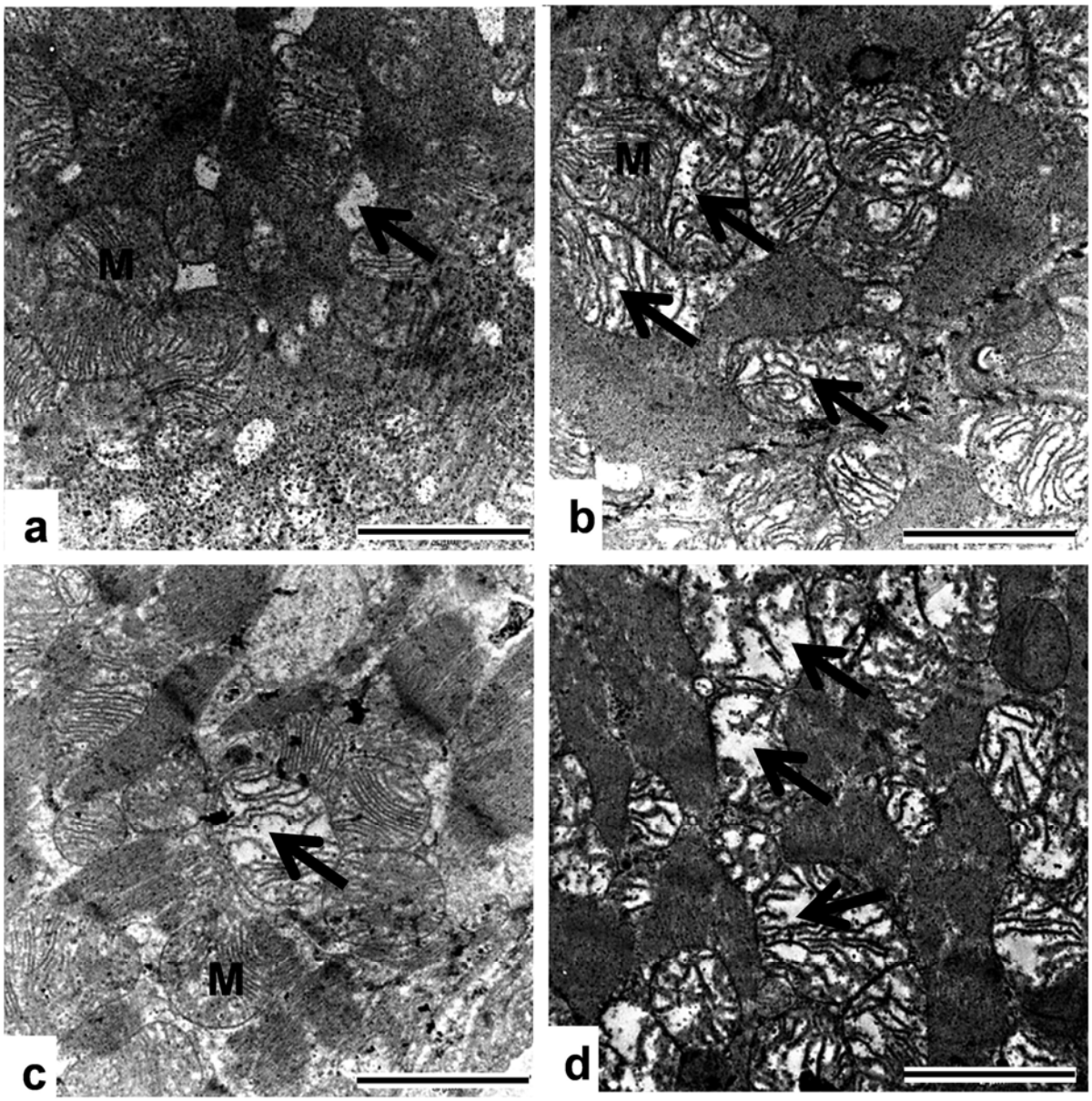

Figure 3: Detailed ultrastructure of mitochondria in transverse sections of the cardiac muscle. Abundant regular cristae are seen in control (a), with axial tubules, a normal feature of healthy cardiac muscle, indicated between the mitochondria (arrow). Damage due to swelling and loss of cristae is evident in experimental groups, found frequently as fragmented cristae (arrows) in Cd (b), less frequently in Hg (c) (arrow), and most frequently and to a higher degree of damage, with complete loss of cristae (arrows) in the Cd+Hg group (d). Normal appearing mitochondria (M). Scale bars = 2 μm.

Mitochondrial damage is a distinguishing features of oxidative stress, and associated autophagy is nescessary for the control of oxidative states. [2, 12] mtDNA lacks protective histones and compared with nuclear DNA has a reduced ability to regenerate, consequently the mitochondria are highly

vulnerable to ROS which can change the number of mitochondria, mtDNA copy number and integrity. Once mtDNA is damaged or mutated, a reduction of antioxidative capacity can further increase ROS production with subsequent oxidative damage. Furthermore, the high lipid content of the mitochondria membranes results in increased levels of oxidative mediated lipid peroxidation [12] that leads to mitochondrial swelling due to increased fluid filtering into the mitochondrial matrix. Structural changes to the mitochondria indicates that these organelles are specific targets of Cd and Hg toxicity, especially for Cd with increased toxicity following co-exposure.

The mitochondria content of cardiac tissue is high and can compensate for minor damage and a loss in function. The number of mitochondria is regulated by the activation of specific transcription factors and signalling pathways [84-86] and an increase is considered an adaptive response to mitochondrial damage and increased need for energy. The formation of large megamitochondria is often associated with free radical generation and are eliminated by mitophagy. [12] In the present study, the mitochondria are swollen, while mega mitochondria were absent.

Dysfunction of the mitochondria, leads to cardiomyocyte apoptosis which which eventually leads to cardiovascular disease. [12] Also associated with oxidative stress is lipid accumulation in cardiac tissue arising from mitochondrial dysfunction. Vacuolization and complete loss of the cristae is a feature of oxidative stress in cardiac tissue and was observed in the Cd and Hg as well as the co-exposure groups.

Some characteristics of autophagy were present in the exposed groups and these are the presence of probably lipid vacuoles and mitochondrial swelling. This protective mechanism occurs via the inhibition of the rapamycin complex 1 (mTORC1) pathway, that prevents endoplasmic reticulum stress. A study investigating Cd and As toxicity as autophagy inducing agents showed that exposure to $CdCl_2$ for up to 18 hrs at doses lower than 10 μM causes autophagy, whereas exposure for 24 hrs

to 1μM $CdCl_2$, caused apoptosis. Cadmium has been shown to induce autophagy via ROS dependant pathways. [45]

Cd activates the necroptosis pathway, [46] resulting in myocardial damage while Hg is a recognized cause of dilated cardiomyopathy. [47, 48] Similar induction of autophagy at low concentrations, followed by necroptosis have been reported for exposure to EtHg. [49] This identifies that autophagy is a cell survival mechanism that occurs at low concentrations for a limited exposure time, after which cytotoxicity and associated apoptosis occurs.

The results of the present study showed that exposure to concentrations of 1000 times the WHO safety limits, with blood concentration of 16,69 nM Cd and 186,67 nM Hg alone and in combination did cause some structural changes to cardiac tissue associated with autophagy, however to conclusively identify autophagy as a mechanism of action, the quantification of biochemical markers associated with this process is necessary.

In typical healthy muscle tissue, collagen distribution is around fibroblasts that synthesize collagen (Fig. 4a) and is also finely dispersed close to the myofibrils and mitochondria, of the endomysium (Fig. 4b). In the heavy metal exposed groups, the collagen deposition is altered when compared to the control. In the Cd group a dense collagen deposition is observed in the endomysium (Fig. 4c) and the interstitium (Fig. 4d), surrounded by damaged mitochondria (Fig. 4d, arrows) and myofibrils. Densely deposited collagen (Fig. 4e) as well as extensive interstitial collagen deposition (Fig. 4f) is also observed in the Hg group. In the co-exposure group (Fig. 4g) extremely thick collagen fibres composed of dense fibrils, that appear to have been directly attached to the muscle fibres (Fig. 4g, arrow) is observed. Collagen deposition around a blood vessel is also observed (Fig. 4h).

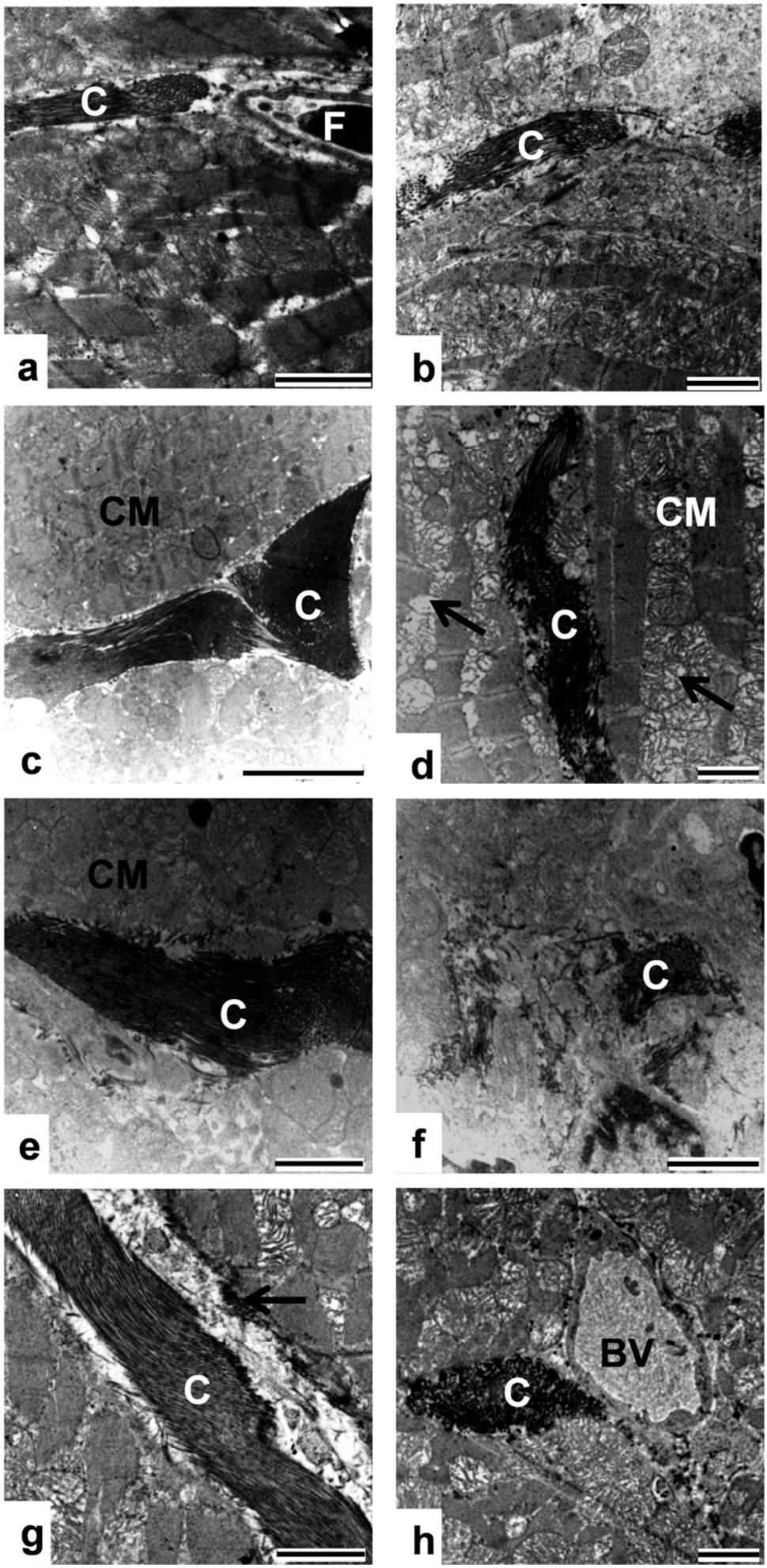
C
F
a
C
b
CM
C
c
CM
C
d
CM
C
e
C
f
C
g
BV
C
h

Figure 4: Ultrastructure of fibrotic collagen in cardiac muscle. Control tissue (a and b) shows normal collagen distribution near a fibroblast (F) in (a) and normal, finely dispersed collagen surrounding mitochondria (b). In the Cd group (c,d) dense accumulation of collagen fibrils is visible in (c) as well as intersitital collagen in (d). Damaged mitochondria in the vicinity are also shown (arrows). Intersitial collagen was also present in the Hg group (e and f), as collagen fibers made up of both densely packed collagen fibrils (e) and loosely dispersed collagen in between mitochondria and muscle fibrils (f). The Cd+Hg group (g and h) had extremely thick fibers made up of dense fibrils of collagen (g), which appears to have been directly attached to the muscle fibrils (arrow), and also collagen in the interstitium (h), in this case shown next to a blood vessel (BV),Collagen (C), Cardiac muscle fibrils (CM). Scale bars = 2 μm.

Myofibroblasts are responsible for collagen turnover under pathological conditions. A fundamental characteristic of hypertensive cardiac remodelling is myocardial stiffness, which is associated with fibrosis, altered contractile and relaxation properties, and changes in cardiac cellularity. [1 4] The most identifying morphological alterations in the remodelling process of heart failure is the accumulation of ECM proteins/fibrosis and myocyte death. [1,4]

Increased interstitial collagen has been identified in Wistar rats exposed to tobacco smoke. [50] These alterations were related to an increase in NOX activity, increased levels of lipid hydroperoxide and depletion of the antioxidant enzymes, CAT, SOD and GPx, implicating the oxidative pathway in ventricular remodelling not associated with inflammation as the cardiac levels of IFN-γ, TNF-α and IL-10 were not different between the groups. [50]

The effects of exposure on the general morphology with H&E staining of the tunica intima, tunica media and tunica adventitia of the aorta was evaluated (Fig. 5). In addition, elastin distribution and arrangement of the fenestrated elastic layers was evaluated using the VvG staining method (Fig. 6). Connective tissue arrangement as well as cell and organelle morphology were evaluated with TEM (Fig. 7).

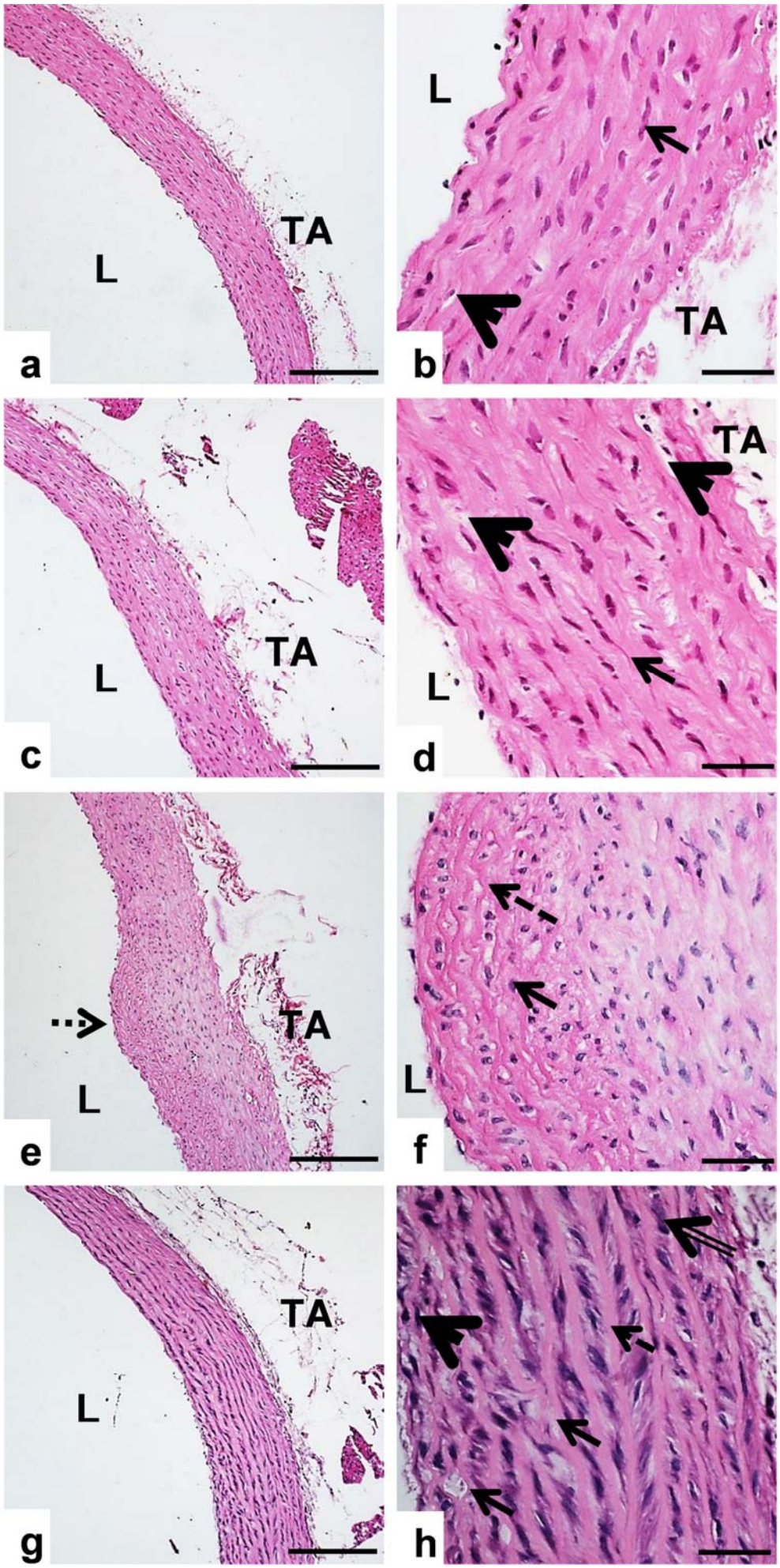
a
L
TA
b
L
TA
c
L
TA
d
TA
L
e
L
TA
f
L
g
L
TA
h

Figure 5: Histology (H&E stain) of the aorta showing the general cell and tissue structure on low (a, c, e and g), and high magnification (b, d, f and h). In the control group (a) showing even thickness throughout the aortic wall and oval nuclei (arrow) with little perinuclear space (arrow head) in (b). The Cd exposed group revealed slight changes in the appearance of the aortic wall (c) as well as flattened nuclei (arrow) and an increase in perinuclear space (arrowhead) in (d). In the Hg group, distortion of the aortic wall is shown in (e) (dashed arrow) and change in tissue structure of the area is visible in (f), with rounded nuclei in the tunica intima (arrow), as well as connective tissue surrounding the cells (dashed arrow). The Cd+Hg group (g and h) revealed some distortion of the arterial wall (g) with a loss of connective tissue banding in the tunica intima (arrow head), flattened nuclei (double arrow) and thick bands of connective tissue (dashed arrow) in the tunica media visible in (h). L = Lumen, TA = Tunica Adventitia, TI = Tunica Intima, TM = Tunica Media. Scale bars (a, c, e, g) = 200 μm, (b, d, f, h) = 40 μm.

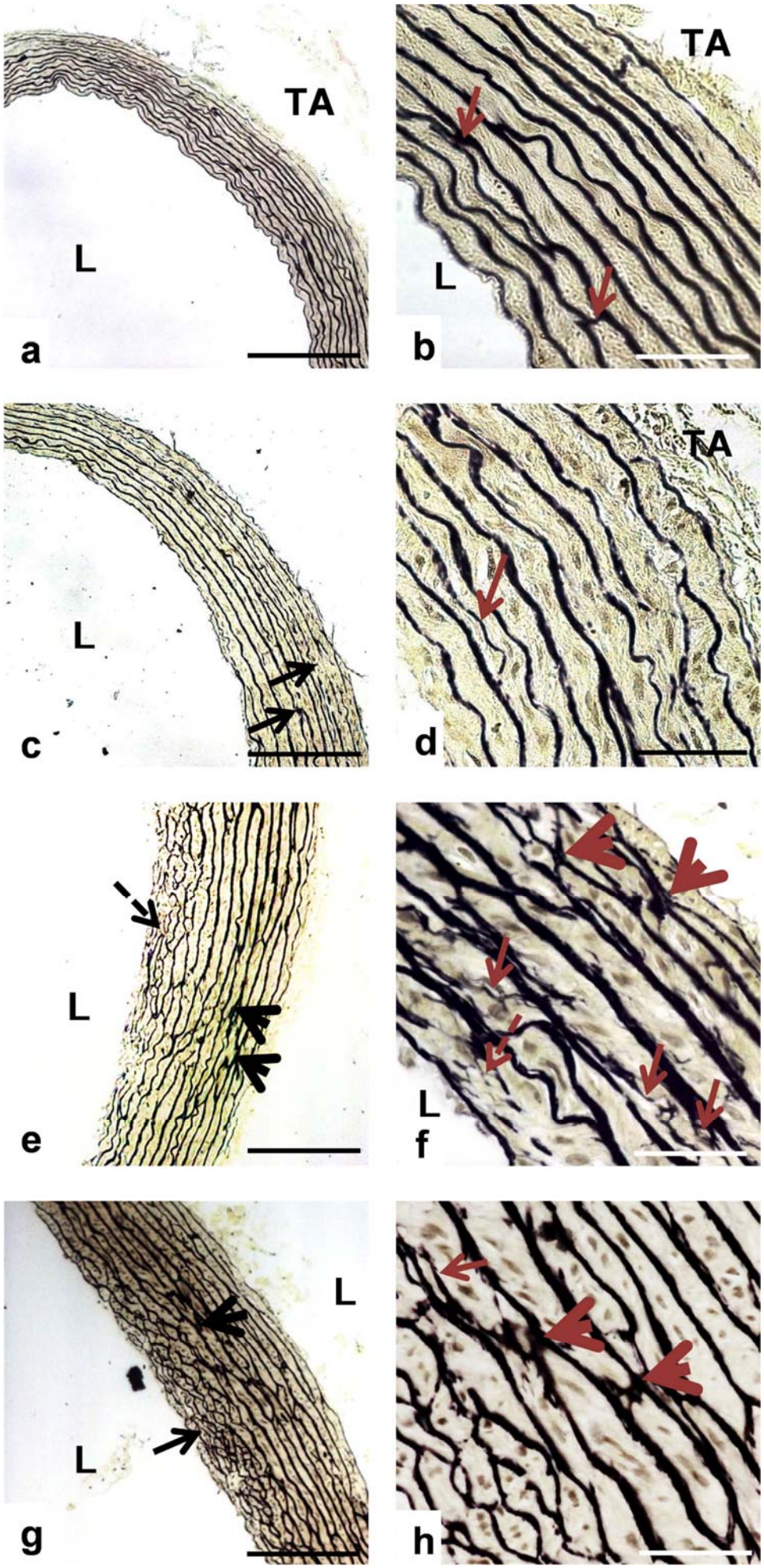
TA
L
a
TA
L
b
L
c
TA
d
L
e
L
f
L
L
g
h

Figure 6: Elastic fibre arrangement in the aorta (VvG stain), on low (a, c, e and g), and high magnification (b, d, f and h).In the control (a and b) aortic wall, evenly thick, regular arranged black staining elastin bands, and interlinkages between elastic laminae are visible in (b) (arrow). The Cd- exposed group (c and d) showed changes in the elastin in areas of thickened aortic wall (c, arrows), with finer elastic fibres between the lamina (d, arrow) and spaces in the lamella visible in (d). Hg group in (e and f) elastin deposition around cells of the tunica intima is present (e, dashed arrow) and increase linkages between the lamina (e, arrowhead). Fine fibre deposition in the Hg group is shown in (f) (arrows) and cross linkages between elastin laminae (f, arrowheads). Cg + Hg group (g and h) showing elastin changes in tunica intima (g, arrow) and large interlinkages between lamina (g and h) (arrow heads). Elastic fibre deposition is present surrounding the cells of the tunica intima (h, dashed arrow). L = Lumen, TA = Tunica Adventitia, TI = Tunica Intima. Scale bars (a, c, e, g) = 20 µm, (b, d, f, g) = 5 µm.

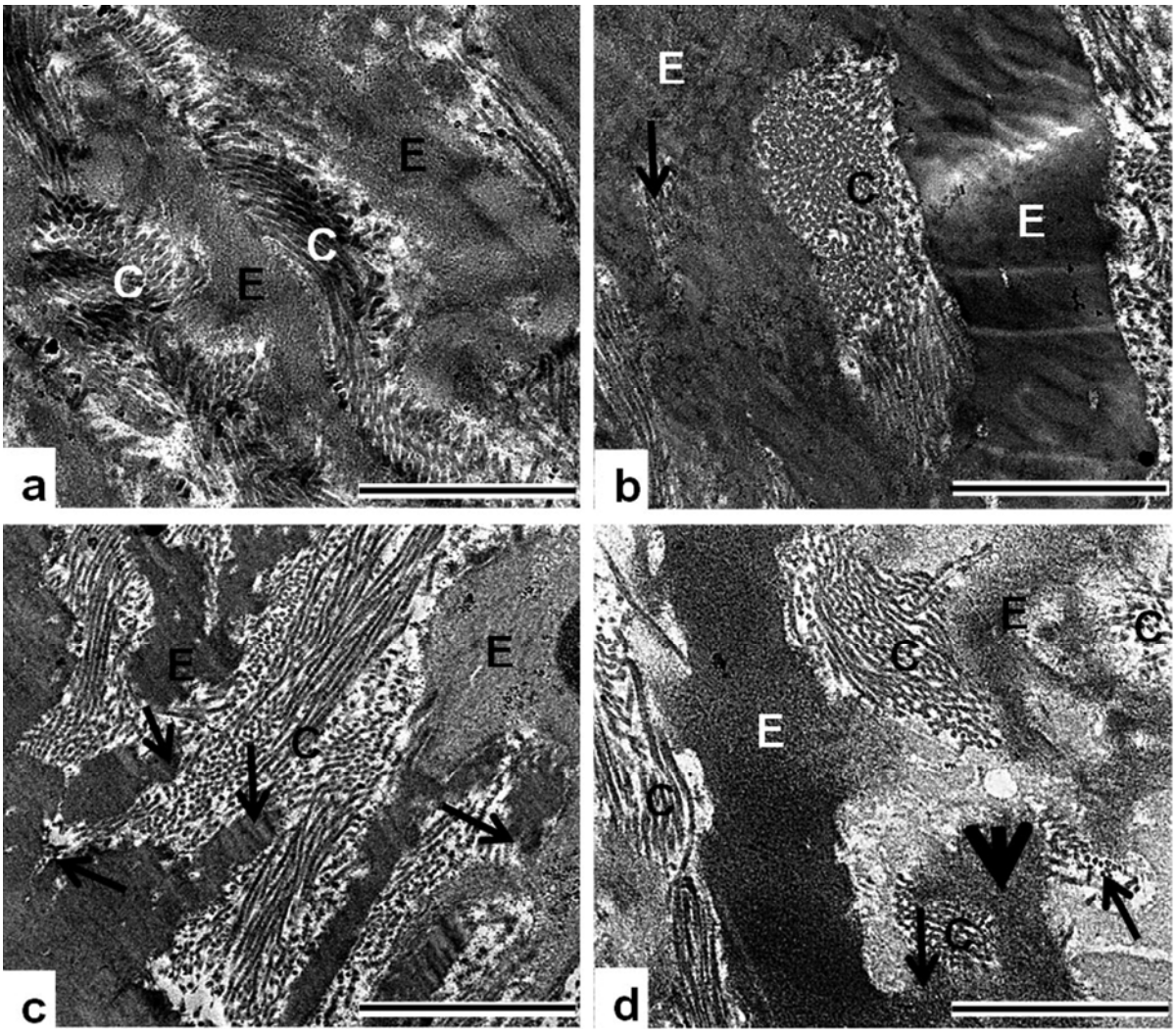

Figure 7: TEM images of the aorta showing differences in the elastin and collagen structure. In (a) control, alternating bands of collagen and elastin are visible. In (b) the Cd group showed collagen deposition in the elastin band (arrow) and elastin fibres with more electron density (E). In the Hg group (c), elastin bands are interrupted (arrows) and collagen fibres are deposited instead. The Cd+Hg group (d) showed elastin fragmentation (arrowhead) and collagen deposition in between the elastin (arrows). C = Collagen, E = Elastin. Scale bars = 2 μm.

In the control group, the thickness of the blood vessel wall was even with the VSMC having oval nuclei (Fig. 5a). Some perinuclear spaces were observed which is a normal feature of tissue shrinkage during processing. Elastin staining revealed smooth, black staining bands of elastin with fibrillar projections forming interlinkages between neighbouring elastic laminae (Fig. 6a and b). In the Cd exposed group, VSMC structure was altered, with the nuclei appearing to be flattened with an increase in the perinuclear space, causing vacuolisation of the aortic matrix. The thickness of the

aortic wall in some areas also appeared increased (Fig. 5c) and at a higher magnification (Fig. 5d) this area contained more connective tissue and cells in the layers of the aorta. Changes to the elastin in the Cd group (Fig. 6c) included a reduction in the wavy appearance of the elastin as well as the presence of finer elastic fibres between the elastic lamina in the thickened areas of the aortic wall (Fig. 6d, arrow). In the Hg group and co-exposure groups, changed to the morphology of the aorta was more apparent and included altered connective tissue structure and cellular arrangement. In the Hg group (Fig. 5e), cell clusters associated with connective tissue that bulges outwards into the lumen was observed. Cell nuclei appeared smaller and rounded, and often bands of connective tissue were observed surrounding the cells. Elastin deposition around the cells of the tunica intima (Fig. 6e dashed arrow), increased in the interlinkages between the lamina and the presence of elastin fibres (Fig. 6f) was observed. The combination group showed similar cellular and connective tissue changes, with a gradual increase in the thickness of the aorta wall (Fig. 5g). For the co-exposed group (Fig. 5h), the nuclei appeared flattened and closer together than observed in the Hg group. The connective tissue appeared to have lost banding definition and instead was surrounded by cells with flattened nuclei, in close proximity to one another. Excessive elastin was present in the tunica intima (Fig. 6g, arrow) as well as large interlinkages between the elastic laminae (Fig. 6h, arrowheads).

Alternating bands of collagen and elastin as typically found in the connective tissue of elastic arteries was observed in the control group (Fig. 7a). Cadmium exposure caused the disruption of the elastic fibres by collagen (Fig. 7b, label C), while an area of new collagen deposition and elastin destruction was observed adjacent to the elastin band (Fig. 7b, arrow). In the Hg exposed group, interruptions in the horizontal elastic bands were observed. In the areas where elastin was lost, collagen was present (Fig. 7c). In the co-exposure group, electron dense elastin strands are present and with areas of lighter density along the main elastin fibre which appears to be newly deposited elastin and similarly arranged elastin is located individually among the collagen bundles (Fig. 7d, thick arrow, label E).

In tunica intima, direct toxicity causes apoptosis of the cells of the endothelium while indirect effects are an increase in cellular proliferation, changes in cellular cell migration and reorganisation, as well as changes to the composition and arrangement of the ECM in the blood vessel walls. [1] The ECM of large blood vessels such as the aorta is composed of elastin and collagen with elastin being the most prominent ECM protein. Elastic fibres in arteries perform the function of energy storage and subsequent release during systole and diastole. A further function is the control the contractibility of VSMC, and is a source of TGF-β, an autocrine factor. [5] Disruption of this process can lead to fibrosis that compromise smooth muscle contractibility.

In contrast, a decrease in collagen degradation also has a profibrotic effect. Collagen degradation is mediated by MMPs which are regulated by hormones, various growth factors and cytokines as well as mechanical strain on the tissue. [1] Although MMPs are involved in collagen degradation, activation can further promote the synthesis of additional collagen in tissues, and therefore creating a positive feedback mechanism for fibrosis. [51, 52] The degradation pathways also often favour the degradation of healthy, intrinsic collagen over newly formed collagen, which in fibrosis is oxidised and highly cross-linked and this results in the accumulation of stiffer collagen. [4,5] In disease levels of myofibroblasts are increased and this causes an increase in the procollagen synthesis and secretion into the pericellular space, where it forms collagen fibrils that assemble into fibres. Functionally, any changes to the ECM components and MMP activity of the myocardium affects the contractile function of myocytes. [3-5] The presence of collagen in smooth muscle has been shown to affect contractility, myocyte mediated signal transduction between cells, as well as growth factor release, the most important of which is TGF – β_1. [53, 54]

Hypertension is also associated with collagen formation in humans as collagen degradation markers and hemodynamic load are reduced after antihypertensive treatment. [1, 3] This has also been confirmed in rat studies. [55] Increased collagen type I synthesis, as was observed in the present study

(data not shown), is a feature of spontaneously hypertensive rats but not in normotensive animals, indicating that increased collagen type I levels in the myocardium are associated with hypertension. [56] Increased collagen cross-linking has also been observed following cardiac hypertrophy in spontaneously hypertensive rats. [57] The suggested pathophysiology is that an increase in systemic blood pressure from arterial modifications affects protein synthesis by cardiomyocytes and fibroblasts which favours increased collagen and total protein synthesis leading to fibrosis [3, 4]

Elastic fibres and SMC function together to allow the dilatory and constrictive action of the arterial wall, recoil ability of elastic blood vessels, and ability to store energy. For elastin formation, the endothelial cells secrete soluble tropoelastin. [3,5] Pericellular deposited microfibrils composed of the protein fibrillin-1 serve as site of aggregation for soluble tropoelastin. [5] In the ECM, elastin is then cross-linked by lysyl oxidase (LOX) and lysyl oxidase like 1 (LOXL1), forming elastin fibres. These elastic fibres first appear as small cell surface globules which over time arrange themselves into larger fibres. [5] In hypertension, in addition to changes in collagen synthesis and deposition, the structure and the processing of elastin, fibrillin, fibronectin and proteoglycans are also altered. [3,5]

Oxidative stress mechanisms have been shown to affect elastin synthesis [5] and in Sprague Dawley rats, as a result of oxidative insult, elastin and increased SMC were observed in the tunica intima creating neointimal tissue masses. [58] Similarly, the present study showed areas of neointimal formation in the groups exposed to Hg (Fig. 5e and f) and the co-exposed group (Fig. 5g and h). Alterations to elastin structure have been reported to decrease arterial compliance. Studies have shown that mice and humans reduced levels of fibulin-5 causes a reduction in arterial compliance, which is correlated with hypertension, reduced cardiac function and an increased risk of death from CVD. [59] In fibulin–5 deficient mice, elastin staining was reduced due to elastin fibres fibre fragmentation visible with electron microscopy.[59] In the present study, for all groups the intensity of the staining was the same. Altered elastin arrangement were observed all groups, with this effect

being the most obvious in the Hg (Fig. 6f) and co-exposed groups (Fig. 6g). Compared with the Hg group, co-exposure to Cd and Hg resulted in increased elastin fibres linking between the lamellae. In contrast, Cd caused interruptions in the elastin lamellae (Fig. 6d), while the presence of collagen bundles (Fig. 7b) possibly contributed to elastic lamellae displacement.

Endothelial cells also contribute to the structural and functional integrity of the vascular wall and damaged endothelial cells are associated with CVD. [1] ROS induces apoptosis of vascular endothelial cells compromising the structural and functional integrity of the endothelium. [1] Exposure to Hg altered the structure of the tunica intima with an increase SMC nuclei (Fig. 5f). Changes to elastin arrangement and structure was observed for all exposed groups (Fig. 6d, f and h) Migration of SMC from the tunica media to the tunica intima occurs as a consequence of endothelial cell damage. [3] An increase in aortic thickness, is the result of SMC proliferation and elastin secretion in the tunica intima of the aortic wall. In addition, disruption of elastin lamella in the tunica media following exposure to Hg and co-exposure to Cd and Hg further contributed changes in the aortic wall. The resulting morphology resembles that of neointimal plaques formed after balloon catheter injury. [60]

Elastin degradation is associated with progressive aortic stiffening that leads to an increase in pulse pressure and a continuous pattern of stiffening effects further increases the risk for cardiovascular events. [3,5] In progeria, premature aging leads to accelerated vascular stiffening or vascular aging. [142] A disordered arrangement of elastin fibres was noted in the current study, presenting as large gaps and irregular connected layers in the metal exposed groups (Fig. 6) indicating that metal exposure is a risk factor for premature arterial aging and the development of CVD.

The histological alterations to VSMC are consistent with endothelial injury and abnormal functioning of the aorta. In the present study, VSMC were more prominent in the tunica media of the Hg and co-exposed groups, while the nuclear shape was altered in all metal exposed groups. Jin

and colleagues [61] reported similar changes that were associated with increased levels of serum endothelin while NO levels were reduced. A balance between endothelin and NO in the endothelium plays a role in maintaining the vascular baseline tension. [1,2] The VSMC proliferation occurs as a result of NO deficiency due to the presence of damaged endothelial cells unable to produce sufficient NO, required for the suppression of VSMC proliferation and growth. Increased VSMC proliferation causes these cells to reach the intima, resulting in the narrowing of the arterial lumen. Reduced NO further contributes to atherosclerotic plaque formation. [2]

In a cell-based study, Cd and Hg was reported to stimulate the proliferation of cultured rabbit aortic smooth muscle cells (ASMC), potentially contributing to the pathogenesis of atherosclerosis and hypertensive disease. [61] A more recent study showed that a long-term exposure of cultured VSMC to low doses of Hg induced vascular remodelling and proliferation through the activation of the MAPK signalling pathways and activation of the inflammatory proteins such as NOX and COX- 2 increased the number of VSMC in the media. Subsequent treatment with COX inhibitors and antioxidants normalized the inflammatory pathways and VSMC proliferation. [62]

Hypertension is a leading risk factor for CVD with the incidence of high blood pressure, increasing over the last three decades. [1,3] Increasingly environmental exposure to metals is being identified as an important risk factor. Increased levels of Cd in urine in an American Indian population were found to be associated with increased blood pressure in comparison to populations with a lower baseline Cd level. [63] Blood pressure variability has been associated with increases in CVD risk, with maladaptive arterial remodelling and increased aortic stiffness being hypothesised as the underlying cause. [64] A meta-analysis of the association between Hg exposure and hypertension found a significant positive correlation. [65] A review of the mechanism underlying the toxicity of the heavy metals Cd, Hg and As suggests that in the case of hypertension and cardiovascular effects, a multiple mechanism for pathogenicity should be considered, due to complexity of the CVS. [66] Hypertensive vascular remodelling is associated with structural and biochemical changes to the

endothelial cells, VSMC and the ECM resulting in vascular remodelling. In this study, continuous exposure to Cd and Hg alone or in combination at relevant dosages may lead to and/or contribute to hypertensive vascular remodelling.

Conclusion

In rats, Cd and Hg at relevant dosages based on the WHO limits for water, induced oxidative related changes to tissue and cellular morphology and these included mitochondrial damage and collagen associated fibrosis. Cd mostly targeted the mitochondria while Hg to a greater degree induced fibrosis. In the aorta, both Cd and Hg also increased collagen deposition detrimentally altered the morphology of fenestrated elastic fibres in the tunica media. Co-exposure resulted in increased cardiotoxicity with increased mitochondrial damage, fibrosis and distortion of the aortic wall due to increased collagen deposition in the tunica media, altered elastin deposition, fragmentation and interlink formation. Exposure to these metals leads to varying degrees to oxidative associated changes to the myocardium and aorta that correlates with a phenotype of premature CVS ageing that is known to lead to hypertension and premature cardiac failure.

Acknowledgements

The authors would like to thank the National Research Foundation for their funding as well as Ms Ilse Janse van Rensburg and other staff members at the University of Pretoria Biomedical Research Centre for their professional assistance with the animal study.

References

[1] Siti, H.N.; Kamisah, Y.; Kamsiah, J. The role of oxidative stress, antioxidants and vascular inflammation in cardiovascular disease (a review). Vasul. Pharm. **2015**, *71*, 40-56.

[2] Steven, S.; `Frenis K.; Oslze, M.; Kalinovic S.; Kuntic, M.; Jimenez, M.T.B.; Vujacic-Mirski, K.; Helmstädter, J.; Kröller-Schön, S.; Münzel, T.; Daiber A. Vascular inflammation and oxidative stress: major triggers for cardiovascular disease. Oxid. Med. Cell. Longev. **2019**

[3] Mikael L.R.; De Paiva, A.M.G.; Gomes, M.N.; Sousa, A.L.L.; Jardim, P.C.B.V.; Vitorino, P.V.O.; Euzébio, M.B.; Sousa, W.M.; Barroso, W.K.S.; Vascular aging and arterial stiffness. Arq. Bras. Cardiol. **2017**, *109*(3), 253-258.

[4] Hinderer, S.; Schenke-Layland, K.; Cardiac fibrosis – a short review of causes and therapeutic strategies. Adv. Drug Deliv. Rev. **2019**, *146*, 77-82.

[5] Cocciolone, A.J.; Hawes, J.Z.; Staiculescu, M.C.; Johnoson E.O.; Mursed, M.; Wagenseil, J.E.; Extracellular matrix in cardiovascular pathophysionlogy. Elastin, arterial mechanics, and cardiovascular disease. Am. J. Physiol. Heart Circ. Physiol. **2018**, *315*, H189-H205.

[6] Rani, A.; Kumar, A.; Lal, A.; Pant, M. Cellular mechanisms of cadmium-induced toxicity: a review. Int. J. Environ. Health Res. **2014**, *24*(4), 378-399.

[7] Navas-Acien, A.; Selvin, E.; Sharrett, A.R.; Calderon-Aranda, E.; Silbergeld, E.; Guallar, E. Lead, cadmium, smoking, and increased risk of peripheral arterial disease. Circulation. **2004**, *109*(25), 3196-3201.

[8] Kaji, T.; Suzuki, M.; Yamamoto, C.; Mishima, A.; Sakamoto, M.; Kozuka, H. Severe damage of cultured vascular endothelial cell monolayer after simultaneous exposure to cadmium and lead. Arch. Environ. Con. Tox. **1995**, *28*(2), 168-172.

[9] Gómez, M.G.; Klink, J.D.C.; Boffetta, P.; Espanol, S.; Sallsten, G.; Quintana, J.G. Exposure to mercury in the mine of Almaden. Occup. Environ. Med. **2007**, *1*, 389-395.

[10] Andreoli, V.; Sprovieri, F.; Genetic aspects of susceptibility to mercury toxicity: An overview. Int. J. Environ. Res. Pub. Health. **2017**, *14.* 93

[11] Genchi, G.; Sinicropi, M.S.; Carocci, A.; Lauria, G.; Catalano, A. Mercury exposure and heart diseases. Int. J. Environ. Res. Pub. Health. **2017,** *14. 74*

[12] Chistiakov, D.A.; Shkurat, T.P.; Melnichenko, A.A.; Grechko, A.V.; Orekhov, A.N. The role of mitochondrial dysfunction in cardiovascular disease: a brief review. Ann. Med. **2018**, *50*(2), 121-127.

[13] Yuan, G.; Dai, S.; Yin, Z.; Lu, H.; Jia, R.; Xu, J.; Song, X.; Li, L.; Shu, Y.; Zhao, X. Toxicological assessment of combined lead and cadmium: acute and sub-chronic toxicity study in rats. Food Chem. Toxicol. **2014**, *65*, 260-268.

[14] Dai, Y.J.; Jia, Y.F.; Chen, N.; Bian, W.P.; Li, Q.K.; Ma, Y.B.; Chen, Y.L.; Pei, D.S. Zebrafish as a model system to study toxicology. Environ. Toxicol. Chem. **2014**, *33*(1), 11-17.

[15] Hounkpatin, A.S.Y.; Edorh, P.A.; Guédénon, P.; Alimba, C.G.; Ogunkanmi, A.; Dougnon, T.V.; Boni, G.; Aissi, K.A.; Montcho, S.; Loko, F.; Ouazzani, N. Haematological evaluation of Wistar rats exposed to chronic doses of cadmium, mercury and combined cadmium and mercury. Afr. J. Biotechnol. **2013**, *12*(23), 3731-3737.

[16] Hounkpatin, A.S.Y.; Johnson, R.C.; Guedenon, P.; Domingo, E.; Alimba, C.G.; Boko, M.; Edorh, P.A. Protective effects of vitamin C on haematological parameters in intoxicated Wistar rats with cadmium, mercury and combined cadmium and mercury. Int. Res. J. Biol. Sci. **2012**, *1*(8), 76-81.

[17] Zeneli, L.; Sekovanić, A.; Ajvazi, M.; Kurti, L.; Daci, N. Alterations in antioxidant defence system of workers chronically exposed to arsenic, cadmium and mercury from coal flying ash. Environ. Geochem. Hlth. **2016**, *38*(1), 65-72.

[18] Gaziano, T.A.; Bitton, A.; Anand, S.; Abrahams-Gessel, S.; Murphy, A. Growing epidemic of coronary heart disease in low-and middle-income countries. Curr. Prob. Cardiology. **2010**, *35*(2), 72-115.

[19] Houston, M.C. The role of mercury and cadmium heavy metals in vascular disease, hypertension, coronary heart disease, and myocardial infarction. Altern. Ther. Health M. **2007**, *13*(2), S128-S133.

[20] Hecht, E.M.; Arheart, K.L.; Lee, D.J.; Hennekens, C.H.; Hlaing, W.M. Interrelation of cadmium, smoking, and cardiovascular disease (from the National Health and Nutrition Examination Survey). Am. J. Cardiol. **2016**, *118*(2), 204-209.

[21] The World Health Organisation. Ten chemicals of major public health concern. Geneva: WHO. 2015. www.who.int/ipcs/assessment/public_health/chemicals_phc/en/. Accessed 22 Nov 2016.

[22] Nair, A.B.; Jacob, S. A simple practice guide for dose conversion between animals and human. J. Basic Clin. Pharmacol. **2016**, *7*(2), 27-37.

[23] Naidoo, S.V.K.; Bester, M.J.; Arbi, S.; Venter, C.; Dhanraj, P.; Oberholzer, H.M. Oral exposure to cadmium and mercury alone and in combination causes damage to the lung tissue of Sprague-Dawley rats. Environ. Toxicol. Phar. **2019**, *69*, 86-94.

[24] Patel, S.S.; Molnar, M.Z.; Tayek, J.A.; Ix, J.H.; Norri, N.; Benner, D.; Heymsfield, S.; Kopple, J.D.; Kovesdy, C.P.; Kalantar-Zadeh, K. Serum creatinine as a marker of muscle mass in chronic kidney disease: results of a cross-sectional study and review of literature. J. Cachexia Sarcopenia Muscle. **2013**, *4*, 19-29.

[25] Mortada, W.I.; Sobh, M.A.; El-Defrawy, M.M.; Farahat, S.E. Reference intervals of cadmium, lead, and mercury in blood, urine, hair, and nails among residents in Mansoura city, Nile Delta, Egypt. Environ. Res. **2002**, *90*(2), 104-110.

[26] Röllin, H.B.; Rudge, C.V.; Thomassen, Y.; Mathee, A.; Odland, J.Ø. Levels of toxic and essential metals in maternal and umbilical cord blood from selected areas of South Africa - results of a pilot study. J. Environ. Monitor. **2009**, *11*(3), 618-627.

[27] Barregard, L.; Sallsten, G.; Fagerberg, B.; Borné, Y.; Persson, M.; Hedblad, B.; Engström, G. Blood cadmium levels and incident cardiovascular events during follow-up in a population-based cohort of Swedish adults: the Malmö diet and cancer study. Environ. Health Persp. **2016**, *124*(5), 594-600.

[28] Leduc, D.; de Francquen, P.; Jacobovitz, D.; Vandeweyer, R.; Lauwerys, R.; de Vuyst, P. Association of cadmium exposure with rapidly progressive emphysema in a smoker. Thorax. **1993**, *48*(5), 570-571.

[29] Matović, V.; Buha, A.; Bulat, Z.; Đukić-Ćosić, D. Cadmium toxicity revisited: focus on oxidative stress induction and interactions with zinc and magnesium. Arch. Ind. Hyg. Toxicol. **2011**, *62*(1), 65-76.

[30] Garner, R.E.; Levallois, P. Cadmium levels and sources of exposure among Canadian adults. Health Rep. **2016**, *27*(2), 10-18.

[31] Jung, E.; Hyun, W.; Ro, Y.; Lee, H.; Song, K. A study on blood lipid profiles, aluminium and mercury levels in college students. Nutr. Res. Pract. **2016**, *10*(4), 442-447.

[32] Lee, S.; Yoon, J.H.; Won, J.U.; Lee, W.; Lee, J.H.; Seok, H.; Kim, Y.K.; Kim, C.N.; Roh, J. The association between blood mercury levels and risk for overweight in a general adult population: results from the Korean National Health and Nutrition Examination Survey. Biol. Trace Elem. Res. **2016**, *171*(2), 251-261.

[33] Simões, M.R.; Azevedo, B.F.; Fiorim, J.; Freire, D.D.; Covre, E.P.; Vassallo, D.V.; dos Santos, L. Chronic mercury exposure impairs the sympathy ovagal control of the rat heart. Clin. Exp. Pharmacol. P. **2016**, *43*, 1038-1045.

[34] Zhao, Z.; Hyun, J.S.; Satsu, H.; Kakuta, S.; Shimizu, M. Oral exposure to cadmium chloride triggers an acute inflammatory response in the intestines of mice, initiated by the over-expression of tissue macrophage inflammatory protein-2 mRNA. Toxicol. Lett. **2006**, *164*(2), 144-154.

[35] Sheikh, T.J.; Patel, B.J.; Joshi, D.V.; Patel, R.B.; Jegoda, M.D. Repeated dose oral toxicity of inorganic mercury in Wistar rats: biochemical and morphological alterations. Vet. World. **2013**, *6*(8), 563-567.

[36] Limaye, D.A.; Shaikh, Z.A. Cytotoxicity of cadmium and characteristics of its transport in cardiomyocytes. Toxicol. Appl. Pharm. **1999**, *154*(1), 59-66.

[37] Ozturk, I.M.; Buyukakilli, B.; Balli, E.; Cimen, B.; Gunes, S.; Erdogan, S. Determination of acute and chronic effects of cadmium on the cardiovascular system of rats. Toxicol. Mech. Method. **2009**, *19*(4), 308-317.

[38] Ghosh, K.; Indra, N. Cadmium treatment induces echinocytosis, DNA damage, inflammation and apoptosis in cardiac tissue of albino Wistar rats. Environ. Toxicol. Phar. **2018**, *59*, 43-52.

[39] Ferramola, M.L.; Pérez Díaz, M.F.; Honoré, S.M.; Sánchez, S.S.; Antón, R.I.; Anzulovich, A.C.; Giménez, M.S. Cadmium-induced oxidative stress and histological damage in the myocardium: effects of a soy-based diet. Toxicol. Appl. Pharm. **2012**, *265*, 380-389.

[40] Baiyun, R.; Li S.; Liu, B.; Lu, J.; Lv, Y.; Xu, J.; Wu, J.; Lv, Z.; Zhang, Z. Luteolin-mediated PI3K/AKT/Nrf2 signalling pathway ameliorates inorganic mercury induced cardiac injury. Exotox. Environ. Safety. **2018,** *161*, 655-661.

[41] Karaboduk, H.; Uzunhisarcikli, M.; Kalender, Y. Protective effects of sodium selenite and vitamin E on mercuric chloride-induced cardiotoxicity in male rats. Braz. Arch. Biol. Technol. **2015,** *58*(2), 229-238.

[42] Prozialeck, W.C.; Edwards, J.R.; Woods, J.M. The vascular endothelium as a target of cadmium toxicity. Life Sci. **2006**, *79*, 1493-1506.

[43] Pearson, C.A.; Lamar, P.C.; Prozialeck, W.C. Effects of cadmium on E-cadherin and VE-cadherin in mouse lung. Life Sci. **2003**, *72*(11), 1303-1320.

[44] Sharma, D.C.; Sharma, P.K.; Sharma, K.K.; Mathur, J.S.; Singh, P.P. Histochemical study of the metabolism and toxicity of mercury. Curr. Sci. **1998**, *57*(9), 483-485.

[45] Son, Y.O.; Wang, X.; Hitron, J.A.; Zhang, Z.; Cheng, S.; Budhraja, A.; Ding, S.; Lee, J.C.; Shi, X. Cadmium induces autophagy through ROS-dependent activation of the LKB1–AMPK signalling in skin epidermal cells. Toxicol. Appl. Pharm. **2011**, *255*(3), 287-296.

[46] Cai, J.; Zhang, Y.; Yang, J.; Liu, Q.; Zhao, R.; Khan, H.; Xu, S.; Zhang, Z. Antagonistic effects of selenium against necroptosis injury via adiponectin–necrotic pathway induced by cadmium in heart of chicken. RCS advances. **2017**, *7*(70), 44438-44446.

[47] Frustaci, A.; Magnavita, N.; Chimenti, C.; Caldarulo, M.; Sabbioni, E.; Pietra, R.; Cellini, C.; Possati, G.F.; Maseri, A. Marked elevation of myocardial trace elements in idiopathic dilated cardiomyopathy compared with secondary cardiac dysfunction. J. Am. Coll. Cardiol. **1999**, *33*(6), 1578-1583.

[48] Rice, K.M.; Walker Jr, E.M.; Wu, M.; Gillette, C.; Blough, E.R. Environmental mercury and its toxic effects. J. Prev. Med. Public Health. **2014**, *47*(2), 74-83.

[49] Choi, J.Y.; Won, N.H.; Park, J.D.; Jang, S.; Eom, C.Y.; Choi, Y.; Park, Y.I.; Dong, M.S. From the cover: ethylmercury-induced oxidative and endoplasmic reticulum stress-mediated autophagic cell death: involvement of autophagosome–lysosome fusion arrest. Toxicol. Sci. **2016**, *154*(1), 27-42.

[50] Rafacho, B.P.; Azevedo, P.S.; Polegato, B.F.; Fernandes, A.A.; Bertoline, M.A.; Fernandes, D.C.; Chiuso-Minicucci, F.; Roscani, M.G.; dos Santos, P.P.; Matsubara, L.S.; Matsubara, B.B. Tobacco smoke induces ventricular remodelling associated with an increase in NADPH oxidase activity. Cell. Physiol. Biochem. **2011**, *27*(3-4), 305-312.

[51] Feldman, A.M.; Li, Y.Y.; McTiernan, C.F. Matrix metalloproteinases in pathophysiology and treatment of heart failure. Lancet. **2001**, *357*, 654-655.

[52] Inokubo, Y.; Hanada, H.; Ishizaka, H.; Fukushi, T.; Kamada, T.; Okumura, K. Plasma levels of matrix metalloproteinase-9 and tissue inhibitor of metalloproteinase-1 are increased in the coronary circulation in patients with acute coronary syndrome. Am. Heart J. **2001**, *141*(2), 211-217

[53] Sorescu, D. Smad3 mediates angiotensin II- and TGF-beta1-induced vascular fibrosis: Smad3 thickens the plot. Circ. Res. **2006**, *98*, 988-989.

[54] Wang, W.; Huang, X.R.; Canlas, E.; Oka, K.; Truong, L.D.; Deng, C.; Bhowmick, N.A.; Ju, W.; Bottinger, E.P.; Lan, H.Y. Essential role of Smad3 in angiotensin II–induced vascular fibrosis. Circ. Res. **2006**, *98*(8), 1032-1039.

[55] Wei, S.; Chow, L.T.; Shum, I.O.; Qin, L.; Sanderson, J.E. Left and right ventricular collagen type I/III ratios and remodelling post-myocardial infarction. J. Card. Fail. **1999**, *5*(2), 117-126.

[56] Díez, J.; Panizo, A.; Gil, M.J.; Monreal, I.; Hernández, M.; Mindán, J.P. Serum markers of collagen type I metabolism in spontaneously hypertensive rats: relation to myocardial fibrosis. Circulation. **1996**, *93*(5), 1026-1032.

[57] Norton, G.R.; Tsotetsi, J.; Trifunovic, B.; Hartford, C.; Candy, G.P.; Woodiwiss, A.J. Myocardial stiffness is attributed to alterations in cross-linked collagen rather than total collagen or phenotypes in spontaneously hypertensive rats. Circulation. **1997**, *96*(6), 1991-1998.

[58] Liaw, L.; Lombardi, D.M.; Almeida, M.M.; Schwartz, S.M.; DeBlois, D.; Giachelli, C.M. Neutralizing antibodies directed against osteopontin inhibit rat carotid neointimal thickening after endothelial denudation. Arterioscler. Thromb. Vasc. Biol. **1997**, *17*(1), 188-193.

[59] Le, V.P.; Yamashiro, Y.; Yanagisawa, H.; Wagensei, J.E. Measuring, reversing and modelling the mechanical changes due to the absence of fibulin-4 in mouse arteries. Biomech. Model Mechan. **2014**, *13*, 1081-1095.

[60] Tran, L.T.; Yuen, V.G.; McNeill, J.H. The fructose-fed rat: a review on the mechanisms of fructose-induced insulin resistance and hypertension. Mol. Cell. Biochem. **2009**, *332*(1-2), 145-149.

[61] Jin, J.J.; Nakura, J.; Zhihong, W.; Yamamoto, M.; Abe, M.; Tabara, Y.; Yamamoto, Y.; Igase, M.; Miki, K.K.T. Association of endothelin-1 gene variant with hypertension. Hypertension. **2003**, *41*, 163-167.

[62] Aguado, A.; María Galán, M.; Olha Zhenyukh, O.; Giulia A.; Wiggers, G.A.; Redondo F.R.R.S.; Peçanha, F.; Martín, A.; Fortuño, A.; Cachofeiro, V.; Tejerina, T.; Salaices M.; Briones A.M. Mercury induces proliferation and reduces cell size in vascular smooth muscle cells through MAPK, oxidative stress and cyclooxygenase-2 pathways. Toxicol. Appl. Pharm. **2013,** *268*(2), 188-200.

[63] Oliver-Williams, C.; Howard, A.G.; Navas-Acien, A.; Howard, B.V.; Tellez-Plaza, M.; Franceschini, N. Cadmium body burden, hypertension, and changes in blood pressure over time: results from a prospective cohort study in American Indians. J. Am. Soc. Hypertens. **2018**, *12*(6), 426-437.

[64] Zhou, G.; Kandala, J.C.; Tyagi, S.C.; Katwa, L.C.; Weber, K.T. Effects of angiotensin II and aldosterone on collagen gene expression and protein turnover in cardiac fibroblasts. Mol. Cell. Biochem. **1996**, *154*(2), 171-178.

[65] Hu, X.F.; Singh, K.; Chan, H.M. Mercury exposure, blood pressure, and hypertension: a systematic review and dose–response meta-analysis. Environ. Health Persp. **2018**, *126*(7), 1-15.

[66] da Cunha Martins Jr, A.; Carneiro, M.F.; Grotto, D.; Adeyemi, J.A.; Barbosa Jr, F. Arsenic, cadmium, and mercury-induced hypertension: mechanisms and epidemiological findings. J. Toxicol. Env. Heal. B. **2018**, *21*(2), 61-82.